Appl. Phys. B 68, 763–766 (1999) / DOI 10.1007/s003409900051

Applied Physics B
Lasers
and Optics

Characterization of photorefractive materials by spontaneous noncolinear frequency doubling

K.-U. Kasemir, K. Betzler

Fachbereich Physik, Universität Osnabrück, Germany
(E-mail: Klaus.Betzler@Physik.Uni-Osnabrueck.de)

Received: 30 October 1998/Revised version: 17 December 1998/Published online: 7 April 1999

Abstract. 'Spontaneous' noncolinear frequency doubling (SNCFD) is a type of optical second-harmonic generation (SHG) that uses scattered light to provide additional fundamental beams in order to accomplish *noncolinear* phase matching. Based on a novel algorithm for the automated evaluation of the resulting ring patterns, we present an easy-to-apply, sensitive, and non-destructive method for the characterization of photorefractive materials, yielding two-dimensional spatial resolution. As applications of the technique, examples for the characterization of lithium niobate crystals are presented.

PACS: 81.70.Dw; 78.20.-e; 42.65.Ky

Photorefractive materials are of extreme interest for applications such as phase conjugation and holographic recording, therefore crystals as for instance lithium niobate ($LiNbO_3$) of excellent homogeneity are required [1]. The properties of $LiNbO_3$ can be tuned in a wide range by varying the composition or by adding appropriate dopants [2–5]. Fabrication of suitable structures also allows for example the realization of a tunable waveguide laser in Ti:Er:$LiNbO_3$ [6]. Means of characterization become increasingly important to achieve reliable reproducibility for the professional development of any device based on photorefractive materials.

Optical characterization methods generally offer excellent accuracy. Of special advantage is optical second-harmonic generation (SHG) which can determine the crystal composition and its spatial variation by measuring phase-matching conditions [7–9]. Here we describe a technique that is based on a unique phase-matching condition for two *noncolinear* fundamental beams. We will then present an algorithm for the automated evaluation of the resulting ring patterns that allows the efficient application of this effect.

Dedicated to Prof. Dr. Eckard Krätzig on the occasion of his 60th birthday.

1 Principles of the method

1.1 Noncolinear frequency doubling

Solving the wave equation for optical frequency doubling (FD) yields the well-known description for the harmonic intensity $I(L, 2\omega)$:

$$I(L, 2\omega) \propto I_1(0, \omega)\, I_1'(0, \omega)\, L^2 \frac{\sin^2(\Delta k\, L/2)}{(\Delta k\, L/2)^2} \,. \qquad (1)$$

It is governed by the intensities $I_{1,1'}$ of the two fundamental beams with frequency ω, the length of the interaction volume L, and the phase mismatch

$$\Delta k = |\boldsymbol{k}_2 - \boldsymbol{k}_1 - \boldsymbol{k}_{1'}| = \frac{4\pi}{\lambda_1}\left(n_2(2\omega) - \frac{n_1(\omega)\cos\varphi + n_1'(\omega)\cos\varphi'}{2}\right) , \qquad (2)$$

with the refractive indices n_i and the angles φ and φ' enclosed by the fundamental wavevectors $(\boldsymbol{k}_1, \boldsymbol{k}_1')$ and the harmonic one $(\boldsymbol{k}_2)$, respectively.

The strongly peaked $(\sin x/x)^2$ behaviour of the second-harmonic intensity implies that the phase matching condition $\Delta k = 0$ can be detected with excellent accuracy. In the case of conventional, colinear FD, (2) is simplified using $\varphi = \varphi' = 0$. Phase matching is usually achieved by temperature tuning, the temperature T_{pm} for noncritical phase-matching is used as the characterizing parameter [10, 11]. In contrast to this, noncolinear FD utilizes two fundamental beams inclined to each other to fulfill the phase-matching condition. Both temperature and angle may then be used in a supplementary way to characterize the material.

In earlier experiments the two necessary fundamental beams were created by splitting the original laser beam and combining the two beams inside the crystal under inspection. The spatial position of the interaction volume in the crystal as well as its expanse can hence be controlled. Using this type

of 'induced' noncolinear frequency doubling (INCFD), three-dimensionally resolved scans of crystal composition can be obtained by measuring the phase-matching temperature at each crystal position for a fixed inclination angle between the two fundamental beams [12]. Providing and controlling the necessary temperatures, however, is time consuming and requires a variable-temperature cryostat or oven into which the crystal has to be installed. Determination of the exact location of the interaction volume can also be tedious, taking into account the temperature dependence of the refractive indices.

1.2 Spontaneous noncolinear frequency doubling

In order to allow swifter measurements at room temperature with the crystal easily accessible on an open carrier, we direct an intense laser beam as the first fundamental $\boldsymbol{k}_1$ perpendicularly onto the crystal surface. While most of the light passes the probe unrefracted, a certain amount is scattered at the crystal surface and also by crystal imperfections, providing second fundamentals $\boldsymbol{k}_1'$. If the angle $\varphi+\varphi'$ between $\boldsymbol{k}_1$ and $\boldsymbol{k}_1'$ fulfills the noncolinear phase-matching condition $\Delta k = 0$ (2), harmonic light ($\boldsymbol{k}_2$) is amplified according to (1) [13].

As $\Delta k = 0$ can be fulfilled in all three dimensions, this 'spontaneous' noncolinear frequency doubling (SNCFD) will produce a cone of harmonic light, visible as a ring pattern when projected onto a screen as sketched in Fig. 1. Numerical evaluations of the phase matching condition for arbitrary directions have proven this ring to be nearly elliptical. For typical electrooptic materials such as $LiNbO_3$, KDP, or $KNbO_3$ the calculated deviation from an ellipse amounts from 10^{-4} degrees ($LiNbO_3$) up to about 10^{-2} degrees ($KNbO_3$), depending on crystal composition and geometry. Compared to the ring broadening discussed in the following paragraph it can be neglected in all practical cases.

Sufficient magnification of the ring pattern reveals a fine structure: The measured intensity of the second-harmonic light depends on φ in a $(\sin x/x)^2$ like manner. According to (2), Δk varies as a function of the angle φ, using (1) we can calculate the *angular* fine structure. Figure 2 shows the excellent match between experimental and calculated data. This structure determines the minimum measurable line width of the SNCFD ring pattern. It varies with crystal composition, crystal size, and scattering geometry. Additionally, it is broadened by inhomogeneities in the samples, but generally it does not render any further deviation of the exact ring pattern from an ellipse.

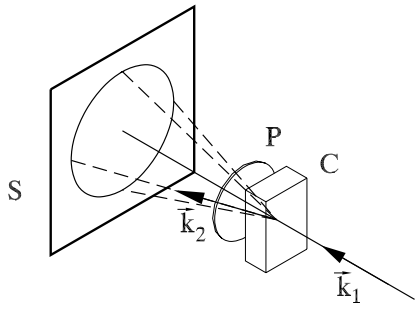

Fig. 1. SNCFD setup; C: crystal, P: projection lens, S: screen, $\vec{k}_i$: wavevectors

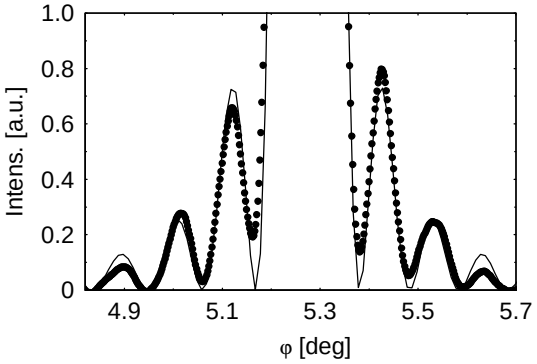

Fig. 2. Fine-structured profile of SNCFD ring; *dots* represent measurement taken from $LiNbO_3$ with 48.7 mol % Li_2O at 250 K, *line* marks calculated dependence

For a plane-parallel slab of $LiNbO_3$ as shown in Fig. 1, ferroelectric c axis aligned vertically, SNCFD can be realized using an ordinarily polarized laser beam directed perpendicular to the crystal face. The horizontal cone angle φ as measured outside the crystal, the so-called SNCFD angle, is then given by:

$$\varphi_{\mathrm{SNCFD}} = \arcsin\left(n_{\mathrm{e}}(2\omega)\sqrt{1-\frac{n_{\mathrm{e}}^2(2\omega)}{n_{\mathrm{o}}^2(\omega)}}\right), \tag{3}$$

with n_{o}: ordinary, n_{e}: extraordinary index of refraction.

Measuring this angle φ_{SNCFD} is often sufficient to determine the composition of materials such as lithium niobate since extensive descriptions of both n_{o} and n_{e} as functions of crystal composition are available [14–17].

1.3 Spatial resolution

With two stepper motors moving the crystal perpendicular to the laser beam in Fig. 1, a two-dimensional scanning setup is realized. The spatial resolution usually is enhanced by focusing the laser beam onto the crystal. The diameter d of a Gaussian beam is commonly defined via the circular area within which the intensity $I(\omega)$ drops to $1/e^2$ of its maximum value. According to (1) this will cause the harmonic intensity $I(2\omega)$ to fall to $1/e^4$, so the SHG-active diameter of the laser beam is smaller than d. As the *effective* laser diameter we therefore define the value that will reduce $I(2\omega)$ by $1/2$:

$$d_{\mathrm{SHG}} = \sqrt{\frac{\ln 2}{4}}\,d \approx 0.41\,d\,. \tag{4}$$

In the case of SNCFD the practically achievable spatial resolution is limited by a previously unknown effect shown in Fig. 3. Graining in addition to the expected broadening. The broadening of the ring pattern is due to the increased divergence of the fundamental beam which is inevitably connected with focusing. This effect in principle could be accounted for in the evaluation of the data. The graining effect yet is due to the random nature of the scattering process: Focusing reduces the scattering volume and thus decreases the number of scattering centers. Consequently the SNCFD ring is partially darkened and distorted, excessive focusing yields an undistinguishable pattern. The effect could be manifested by an

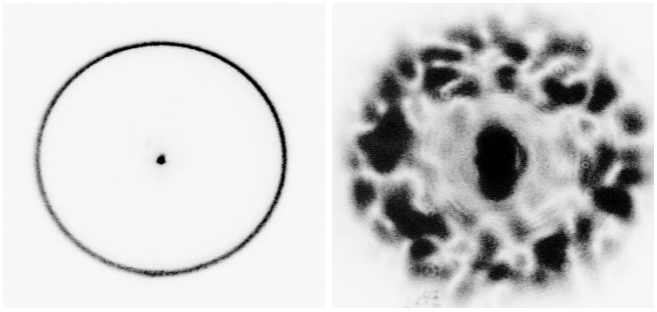

Fig. 3. SNCFD ring pattern, influence of focusing the fundamental laser beam; effective diameter of fundamental beam according to (4) is 300 μm (*left*) versus 15 μm (*right*)

appropriate numerical simulation [18]. The highest practicable spatial resolution reached so far is $d_{\mathrm{SHG}} \approx 30\,\mu\mathrm{m}$.

1.4 Automated ring detection

A CCD camera in combination with a frame-grabber card records the ring images from the rear side of the ground-glass screen in Fig. 1. As a two-dimensional spatially resolved scan of the crystal results in up to some thousand ring pictures, it is necessary to use an automatic evaluation algorithm for the ring parameters.

To extract the essential ring information from the images, the hough transformation [19] into the parameter space of an ellipse with center coordinates (x_0, y_0), horizontal radius r, and eccentricity e is applied to the original picture:

$$(x - x_0)^2 + \frac{1}{e^2}(y - y_0)^2 = r^2 \,. \tag{5}$$

To implement this transformation in the full four-dimensional parameter space would be very time and memory consuming, therefore the hough transformation is combined with a suitable optimization strategy. The transformation is calculated for fixed values of (x_0, y_0) to reduce the computational requirements for memory and time; thus only a two-dimensional transformation into $\{r, e\}$-space has to be calculated. In order to find the correct ellipse center, the differential evolution method [20] is used to vary center coordinates until the hough transformation produces an optimum result [21].

2 Example applications

The possibilities of the new characterization technique are demonstrated by three application examples concerning lithium niobate crystals. This material was chosen as a relatively complete description of the refractive indices for pure and doped lithium niobate is available [14–17]. Using this Sellmeier-type description, the measured SNCFD angles can be directly referred to composition values.

2.1 Experimental details

The measurements were carried out using a Q-switched Nd:YAG laser as fundamental light source with a pulse length of 70 ns, adjustable peak power of 1 . . . 10 kW, and repetition rate of 1 kHz. With the fundamental wavelength of 1064 nm of the Nd:YAG laser, SNCFD rings with cone angles between 5° and 20° are generated in lithium niobate, depending on its composition. The crystal samples on which the measurements were performed had a thickness of 1 . . . 2 mm, the two other spatial dimensions are indicated in the figures. The second-harmonic rings were detected with a slow-scan video camera connected to a frame-grabber card, the integration time for each picture was typically 0.1 s. A complete two-dimensional scan of a crystal can thus be performed in several minutes. Considerably more time has to be spent for the numerical evaluation of the ring parameters: with a state-of-the-art personal computer the evaluation of one ring takes approximately 10 s.

2.2 Competitive factors

The technique presented is very sensitive to slight changes in the refractive indices. To draw certain conclusions from the measurements, all factors influencing the refractive indices of the material under inspection must be carefully taken into account. In *photorefractive* materials such as lithium niobate, the photorefractive effect may contribute to refractive index changes. Its contribution is intensity dependent, thus its influence has to be ruled out by a variation of the laser intensity. The same holds for *thermal effects*: a variation of the fundamental beam intensity must not yield any changes in the results, i.e. the measured SNCFD angle. In *thermally treated* (reduced/oxidized) crystals, surface effects have to be considered in their influence on the (integrated) index. If surface effects cannot be neglected, a three-dimensional technique [12] is to be preferred or should be used as a complement.

2.3 Homogeneous lithium niobate

To show the excellent sensitivity provided by SNCFD, a highly homogeneous sample was investigated, namely $LiNbO_3$ grown from a melt containing a certain amount of potassium [22]. As can be derived from Fig. 4, composition changes of less than 0.01% Li_2O can be resolved by the method.

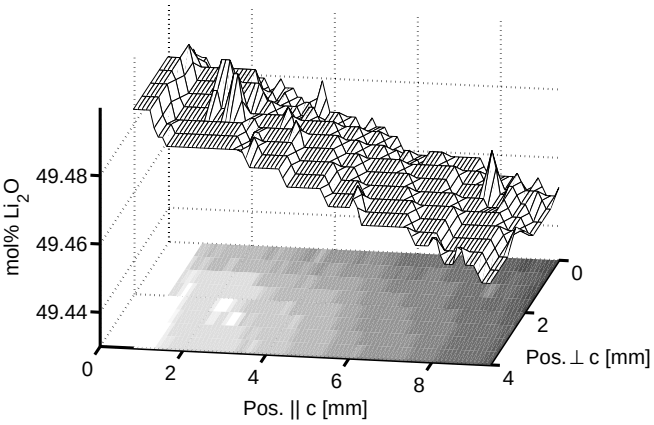

Fig. 4. SNCFD topography of a highly homogeneous $LiNbO_3$ crystal grown from a potassium-enriched melt, revealing a slight variation of crystal composition in the direction of growth (*c* axis)

2.4 VTE-treated lithium niobate

The composition of $LiNbO_3$ crystals (Li/Nb ratio) can be adjusted after the growth process by thermal treatment in an appropriate Li_2O- or Nb_2O_5-enriched atmosphere (vapor transport equilibration – VTE) [23, 24]. SNCFD measurements are an excellent tool to monitor the treatment. As an example the composition topography of a congruently grown $LiNbO_3$ crystal after a comparably short VTE treatment of 400 h is shown in Fig. 5. The measurements were carried out on a 1.5-mm-thick platelet cut out of the middle of a larger VTE-treated lithium niobate crystal. To get a better survey, the composition topography of only half of the platelet is sketched in Fig. 5.

2.5 Magnesium-doped lithium niobate

Doping $LiNbO_3$ with magnesium is known to reduce the so-called optical damage considerably [25]. Yet congruently grown Mg-doped crystals exhibit growth striations, the nature of which is not quite clear [26]. Whereas via other methods the striations can only be detected qualitatively, SNCFD allows a quantitative description. A two-dimensional SNCFD scan of a typical crystal with striations is shown in Fig. 6. The measured topography can be referred to a Mg content of 3.7 mol % in congruent $LiNbO_3$ with variations of ± 0.1 mol % or – if the Mg content is assumed to be constant – to variations in the Li content (extrapolated to 48.5 mol %) of ± 0.01 mol %.

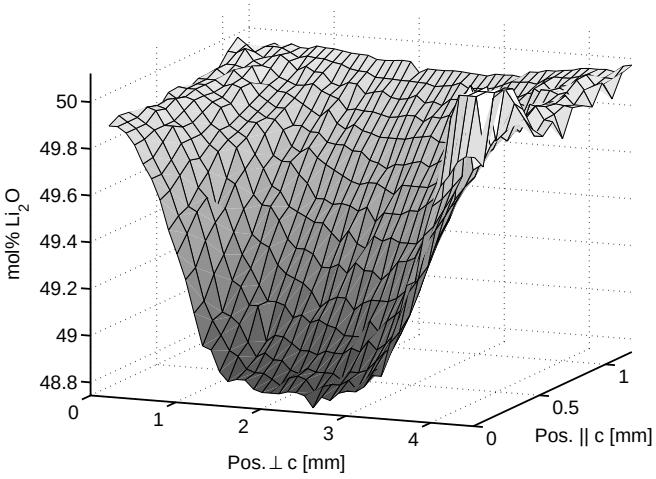

Fig. 5. SNCFD topography of a VTE-treated $LiNbO_3$ crystal. At the crystal borders (*left*, *right*, and *rear side*) a nearly stoichiometric composition of the crystal is reached by the treatment

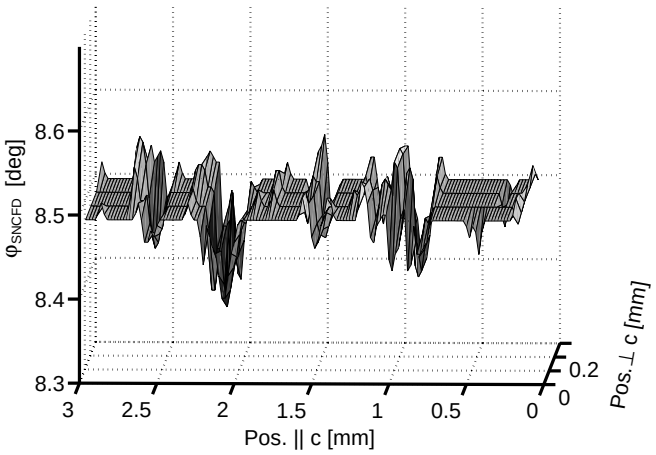

Fig. 6. Striation topography in a Mg-doped lithium niobate crystal measured by SNCFD. 'Plains' indicate regions of constant composition, 'valleys' a deficit of Mg or Li, 'mountains' a respective surplus

3 Conclusion

Spontaneous noncolinear frequency doubling offers a very sensitive method for the characterization of crystals. Although the experimental effort is very small, spatial resolution for two-dimensional topographical inspection of the crystal composition is comparable to other methods [27]. The presented algorithm performs automated evaluation of the huge number of resulting ring patterns, turning the physical effect of SNCFD into a valuable tool for research and development.

Acknowledgements. We are indebted to Dr. B.C. Grabmaier, Prof. S. Kapphan, and Dr. E.P. Kokanyan for providing the test crystals. Financial support from the Deutsche Forschungsgemeinschaft (SFB 225, A 10) is gratefully acknowledged.

References

1. K. Buse, A. Adibi, D. Psaltis: Nature **393**, 665 (1998)
2. D.A. Bryan, R. Gerson, H.E. Tomaschke: Appl. Phys. Lett. **44**, 847 (1984)
3. T.R. Volk, V.I. Pryalkin, N.M. Rubinina: Opt. Lett. **15**, 996 (1990)
4. T.R. Volk, N.M. Rubinina: Ferroel. Lett. **14**, 37 (1992)
5. J.K. Yamamoto, K. Kitamura, N. Iyi, S. Kimura, Y. Furukawa, M. Sato: Appl. Phys. Lett. **61**, 2156 (1992)
6. K. Schäfer, I. Baumann, W. Sohler, H. Suche, S. Westenhöfer: IEEE J. Quantum Electron. **QE-33**, 1636 (1997)
7. H. Fay, W.J. Alford, H.M. Dess: Appl. Phys. Lett. **12**, 89 (1968)
8. N. Schmidt, K. Betzler, B.C. Grabmaier: Appl. Phys. Lett. **58**, 34 (1991)
9. M. Wöhlecke, G. Corradi, K. Betzler: Appl. Phys. B **63**, 323 (1996)
10. N. Schmidt, K. Betzler, S. Kapphan: Cryst. Latt. Def. Amorph. Mater. **15**, 103 (1987)
11. Chr. a. d. Horst, K.-U. Kasemir, K. Betzler: J. Appl. Phys. **84**, 5158 (1998)
12. A. Reichert, K. Betzler: J. Appl. Phys. **79**, 2209 (1996)
13. J.A. Giordmaine: Phys. Rev. Lett. **8**, 19 (1962)
14. U. Schlarb, K. Betzler: Phys. Rev. B **48**, 613 (1993)
15. U. Schlarb, K. Betzler: Phys. Rev. B **50**, 751 (1994)
16. K.-U. Kasemir, K. Betzler, B. Matzas, B. Tiegel, M. Wöhlecke, N. Rubinina, T. Volk: Phys. Status Solidi A **166**, R7 (1998)
17. K.-U. Kasemir, K. Betzler, B. Matzas, B. Tiegel, T. Wahlbrink, M. Wöhlecke, B. Gather, N. Rubinina, T. Volk: J. Appl. Phys. **84**, 5191 (1998)
18. K.-U. Kasemir: PhD Thesis, Osnabrück University (1998)
19. P.V.C. Hough: U.S. Patent 3069654 (1962)
20. K. Price, R. Storn: Dr. Dobb's J. **4**, 18 (1997)
21. K.-U. Kasemir: unpublished
22. G.I. Malovichko, V.G. Grachev, E.P. Kokanyan, O.F. Schirmer, K. Betzler, B. Gather, F. Jermann, S. Klauer, U. Schlarb, M. Wöhlecke: Appl. Phys. A **56**, 103 (1993)
23. Y.S. Luh, M.M. Fejer, R.L. Byer, R.S. Feigelson: J. Cryst. Growth **85**, 264 (1987)
24. D.H. Jundt, M.M. Feijer, R.L. Byer: IEEE J.Quantum Electron. **QE-26**, 135 (1990)
25. R.L. Byer, Y.K. Park, R.S. Feigelson, W.L. Kway: Appl. Phys. Lett. **39**, 17 (1981)
26. B.C. Grabmaier, F. Otto: J. Cryst. Growth **79**, 682 (1986)
27. H. Jones-Bey: Laser Focus World **9**, 32 (1997)